

Two interacting particles in a disordered chain IV: Scaling of level curvatures

André Wobst and Dietmar Weinmann^a

Institut für Physik, Universität Augsburg, 86135 Augsburg, Germany

October 17, 2018

Abstract. The curvatures of two-particle energy levels with respect to the enclosed magnetic flux in mesoscopic disordered rings are investigated numerically. We find that the typical value of the curvatures is increased by interactions in the localised regime and decreased in the metallic regime. This confirms a prediction by Akkermans and Pichard (Eur. Phys. J. B **1**, 223 (1998)). The interaction-induced changes of the typical curvatures at different energies and disorder strengths exhibit one-parameter scaling with a conductance-like single parameter. This suggests that interactions could influence the conductance of mesoscopic systems similarly.

PACS. 71.10.-w Theories and models of many electron systems – 71.30.+h Metal-insulator transitions and other electronic transitions – 73.20.Jc Delocalisation processes

1 Introduction

For disordered mesoscopic systems, the curvatures of one-particle energy levels as a function of an external parameter like the magnetic flux enclosed by a system with ring geometry have been studied intensively since Edwards and Thouless [1, 2] proposed that the typical value of the curvatures should be closely related to the non-interacting conductance. Intuitively, it is clear that level curvatures and the conductance should be related. Since the effect of an enclosed flux is equivalent to generalised boundary conditions, the curvatures measure the sensitivity of the energy levels with respect to the boundary conditions. Obviously, eigenstates which are localised are affected much less by the boundaries than extended states and the level curvatures are strongly reduced by localisation. The argument given by Edwards and Thouless is based on the occurrence of momentum matrix elements in a perturbative expansion of the flux dependence of the eigenenergies as well as in the Kubo formula for the conductance. It follows that the dimensionless conductance g_1 should be proportional to the typical curvature \bar{c} divided by the mean level spacing Δ_1 . Several analytical studies support this Thouless relation, and it has also been verified numerically within the Anderson model [3]. The mean of the absolute value of the curvatures is indeed proportional to a properly defined conductance in the ballistic and the diffusive regime whereas in the localised regime, the mean of the logarithms of curvatures and conductance were found to be proportional. In addition, it is known that the energy level statistics at fixed flux also contains an energy scale

(the so-called Thouless-energy), which is proportional to the typical one-particle curvature and thus to the conductance.

Furthermore, it was shown that not only the mean value of the curvatures but also their distribution depends on the conductance. In the diffusive regime [4, 5, 6], the distribution is very close to that obtained from random matrix theory for the Gaussian orthogonal ensemble (GOE) [7] while a log-normal distribution is approached in the localised regime [3, 4, 5, 8].

Although the relation between curvatures and conductance has been intensively studied in the non-interacting case, very little is known about the relevance of the curvatures of many-body levels in disordered systems with electron-electron interactions. Only persistent currents which are related to the first derivative of the many-body ground state energy with respect to flux have been studied in detail in the presence of interactions [9, 10]. Several theories predict an enhancement of persistent currents due to interactions. Recently, very strong enhancement has been found for spinless fermions in individual one-dimensional rings at large disorder strength [11]. However, it is not yet clear whether this can fully account for the experimental findings in the diffusive regime which suggest values up to two orders of magnitude larger than the predictions of theories neglecting interactions.

The interplay of disorder and interaction is a subject of very intense research activities [10]. While perturbative approaches can be used for weak disorder or weak interaction strength in the thermodynamic limit, a relatively new approach considers a small number of particles with both, strong disorder and strong interaction. It has been predicted [12, 13] and confirmed numerically [14, 15, 16] that a

^a e-mail: Dietmar.Weinmann@Physik.Uni-Augsburg.DE

short-range interaction enhances the localisation length of certain two-particle states in disordered systems. However, energy dependent studies for quasi-particles have shown that the effect is suppressed at small excitation energies [17].

Since this enhancement effect can be connected to the two-particle energy level statistics [18], the latter has been investigated in detail. In the non-interacting case, two-particle energies are sums of two one-particle energies, and therefore the two-particle level spacing distribution is always close to the uncorrelated Poisson distribution, even in metallic systems where the one-body level statistics is close to the universal Wigner-Dyson statistics for the GOE. In contrast, the presence of interactions leads to spectral correlations with interesting properties. For on-site interactions on a one-dimensional lattice, there exists a duality transformation which maps the behaviour at weak interaction to the one at very strong interaction [19, 20]. Therefore, the spectrum at infinite interaction is uncorrelated like in the non-interacting case. Maximal correlations occur for intermediate interaction strength. In the band centre, these correlations are very close to the critical ones found in several other systems exhibiting weak chaos like the Anderson model in three dimensions at the critical point [21]. The appearance of the critical statistics for two interacting particles [19] is accompanied by multi-fractal wavefunctions. This may be caused by the multi-fractal structure of the interaction matrix itself [22].

While the spectral correlations seem to be closely related to the interaction-induced enhancement of the localisation length in the localised regime [18], it is less obvious whether and how they can be used to predict observable quantities like the conductance of metallic samples. It is therefore necessary to consider properties of the two-particle system which are more directly connected to the mobility of the particles. An important step in this direction is a numerical study of the real-time development of two-particle wave-packets [23], where the time-dependence of the spreading of two particles released at adjacent sites is observed, yielding useful informations on the influence of the interactions. While they reduce the speed of the ballistic spreading of the wave-packet at very short times, they lead on the other hand to an extension beyond the one-particle localisation length L_1 for intermediate times and the larger two-particle localisation length L_2 is reached sub-diffusively after very long time [23]. While long times yield informations about the localised regime, the short time dynamics should be connected to the behaviour of metallic samples.

The level curvatures with respect to an external parameter like an enclosed flux represent a static quantity which is directly related to the mobility of the particles in metallic and in insulating samples. Very recently, Akkermans and Pichard [24] have studied the connection between spectral correlations and level curvatures for two interacting particles. They predicted that the curvatures should be enhanced by interactions in localised and reduced in metallic samples. However, the analytic arguments used to obtain this very interesting result contain

crude approximations and it is not obvious how to extract details like the curvature distributions or the energy dependence and information about the crossover between the two regimes. This has motivated us to perform a numerical study of the two-particle level curvatures in a one-dimensional ring. We have unambiguously confirmed the prediction mentioned above [24]. Furthermore, our data suggest that the effect of the interaction on curvatures exhibits one-parameter scaling. The scaling parameter is closely related to the non-interacting conductance. Many of the observed features are closely related to the spectral statistics and the dynamics of wave-packets studied in the preceding papers [19, 22, 23] of this series on two interacting particles in a disordered chain.

After introducing the system in Section 2, we explain in Section 3 our numerical techniques and discuss different averaging procedures. The results for the effect of the interaction on the typical level curvatures are presented in Section 4. Details of the curvature distribution are shown in Section 5 before we present our conclusions.

2 Disordered ring

The Hamiltonian for two interacting particles can be written in the form

$$H = H_1 \otimes \mathbf{1} + \mathbf{1} \otimes H_1 + H_{\text{int}}. \quad (1)$$

H_1 describes one particle in a disordered chain with L sites and reads

$$H_1 = \sum_{n=0}^{L-1} \left(-t|n+1\rangle\langle n| - t^*|n\rangle\langle n+1| + V_n|n\rangle\langle n| \right), \quad (2)$$

where $|n\rangle$ is a Wannier function localised at site n . Periodic boundary conditions close the chain to a ring, implying $|n\rangle \equiv |n+L\rangle$. The disorder is modeled by random on-site energies V_n which are distributed uniformly inside the interval $[-W : W]$. The nearest neighbor hopping matrix elements

$$t = t_0 \exp(2\pi i \phi/L), \quad (3)$$

whose absolute value t_0 is set to unity and defines the energy scale, contain the dimensionless flux $\phi = \varphi/\varphi_0$ which is given by the magnetic flux φ threading the ring in units of the flux quantum $\varphi_0 = hc/e$. The magnetic flux affects only the phase of the hopping matrix elements t and can be transformed by a gauge transformation into a generalised periodic boundary condition with a phase shift of $2\pi\phi$. Therefore, a variation of the magnetic flux is equivalent to a change of the boundary condition. For the one-particle case the curvatures

$$c_\alpha = \left. \frac{\partial^2 \epsilon_\alpha}{\partial \phi^2} \right|_{\phi=0} \quad (4)$$

of the eigenvalues ϵ_α of H_1 are directly related to the conductance by means of the Thouless relation.

For simplicity, we use a Hubbard-like on-site interaction with strength U between the two particles described by

$$H_{\text{int}} = \sum_{n=0}^{L-1} U |nn\rangle\langle nn|. \quad (5)$$

Here, $|mn\rangle$ means $|m\rangle|n\rangle$ and restricting ourselves to the case of two fermions with opposite spins, the dimension of the Hilbert space is $M = L(L+1)/2$. A complete basis for the symmetric configuration space part of the states is given by

$$\begin{aligned} |mn\rangle_s &= \frac{1}{\sqrt{2}}(|mn\rangle + |nm\rangle) \quad \text{for } m \neq n \\ |nn\rangle_s &= |nn\rangle. \end{aligned} \quad (6)$$

3 Numerical techniques

3.1 Computation of level curvatures

We write the Hamiltonian (1) in the symmetric two-particle basis (6). Since the resulting $M \times M$ matrix is very sparse, we use the Lanczos algorithm to numerically calculate the full set of M two-particle eigenenergies.

The absolute values of the curvatures of different levels (even within the same disorder realisation) usually differ by many orders of magnitude, making it difficult to obtain reliable numerical results for small as well as for large curvatures. Therefore we calculate the two-particle eigenenergies at several values of the magnetic flux between $\phi = 0$ and $\phi \sim 10^{-3}$. For each of the M eigenvalues, we first estimate the fourth derivative with respect to the flux. Then, we perform a least square fit with a parabola to the calculated data. The weights of the data points at different flux values are adjusted individually for each of the eigenvalues as a function of the estimates for the fourth derivative and the typical inaccuracy of the numerically calculated eigenvalues [25].

Another possibility is to use the perturbative expression for the eigenenergies in second order in the magnetic flux. This allows to calculate the curvatures directly and without the errors arising from the numerical calculation of derivatives. However, this requires the eigenenergies and in addition all of the eigenvectors of the Hamiltonian matrix at $\phi = 0$. Since this considerably increases the computation time and required memory, we have not used this approach for the large matrices occurring in the interacting problem. However, in the one-particle case such a calculation is easily possible for the ring sizes we consider and we have used this to adjust our general method and to verify its precision by comparing two-particle results without interaction. We believe that this yields a good estimate for the precision of the curvatures calculated at arbitrary interaction strength.

3.2 Averaging procedures

Since we want to discuss typical values of the curvatures as a function of disorder and interaction strength, the averaging technique must be chosen carefully. Besides the mean

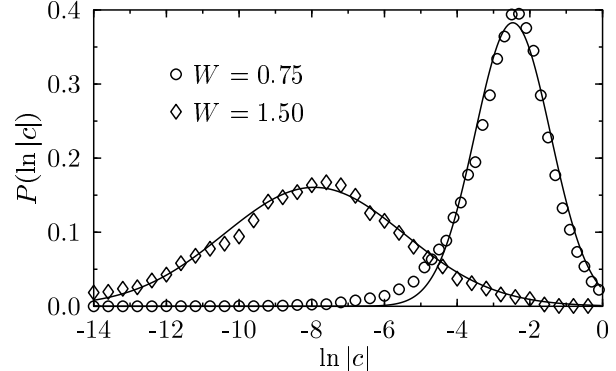


Fig. 1. Typical distributions $P(\ln |c|)$ of curvatures for two-particle levels in the energy interval $[-2.5 : -1]$ at interaction strength $U = 0.5$ and ring size $L = 100$. The solid lines are Gaussian fits.

of the absolute values and the mean of the logarithm of the absolute values, we have used another way to extract a typical curvature, exploiting the fact that there is a peak in the distribution $P(\ln |c|)$ as shown in Figure 1 and a fit of a log-normal distribution is usually rather good. Such a log-normal curvature distribution has been observed numerically in the insulating regime of the Anderson model [3, 4, 5] and was derived analytically for one-dimensional disordered rings [8]. The peak width grows with the disorder strength and the position of the maximum decreases. This is reminiscent of the behaviour of one particle in a two-dimensional disordered system in the localised regime where the dimensionless conductance g_1 is log-normally distributed with typical value $\langle \ln g_1 \rangle \propto -L/L_1$ with a variance which is given by the mean value $-\langle \ln g_1 \rangle$ [26]. Our data for the curvatures are rather well approximated by the estimate $\langle \ln |c| \rangle = \ln(4\pi^2 \Delta_1) - L/L_1$, where Δ_1 denotes the average one-particle level spacing and also show a variance close to $-\langle \ln |c| \rangle$. We found that the most reproducible results for typical curvatures are obtained by fitting the distribution of curvatures (rather than computing averages) because this minimises the influence of the statistically less accurate points in the tails of the distribution. We always used a log-normal fit for this purpose as shown in Figure 1, yielding numerically reliable results for the average $\langle \ln |c| \rangle$ and introduce $\tilde{c} = \exp(\langle \ln |c| \rangle)$ as a typical curvature. Additionally, we qualitatively confirmed our results using the numerically less stable direct averages of $\ln |c|$ and $|c|$.

4 Typical curvatures

4.1 Energy dependence without interaction

The energy dependence of the typical two-particle level curvature is shown in Figure 2. In order to understand the non-interacting curve (full symbols), let us first recall the energy dependence of the curvatures of one-particle levels in one-dimensional rings. In the average over disorder realisations the curvatures are small at the band edges

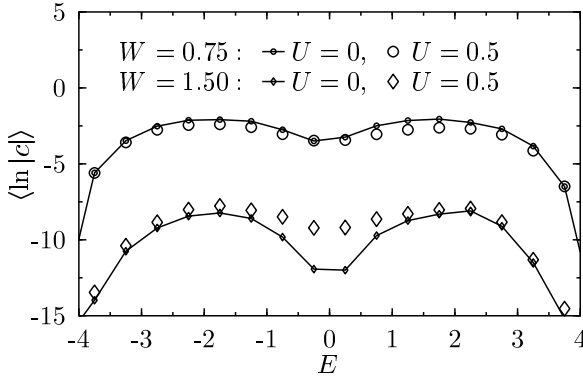


Fig. 2. The energy dependence of typical curvatures for different disorder strengths W and $L = 100$. $\langle \ln |c| \rangle$ is plotted for the cases without (full symbols, connected by lines) and with interaction $U = 0.5$ (open symbols).

but several orders of magnitude larger in the band centre. Their sign is alternating with the number of the state. In the non-interacting two-particle case different regions can be observed. The edges at large absolute energy close to the band edges at $|E| = 2(2t_0 + W)$ arise from one-particle states where both of the particles are close to the same edge of the one-particle band where their typical curvature is very small. Therefore the two-particle level curvatures are small at the band edges. To obtain a state in the centre of the two-particle band, there are several possibilities to combine two one-particle states such that their total energy is close to $E = 0$. They can be chosen at the two opposite edges of the one-particle spectrum, both having small one-particle curvature and therefore yielding a small two-particle curvature. The other extreme is represented by both particles occupying states close to the middle of the one-particle band. Then the individual curvatures are much larger but may have different sign. The typical two-level curvature in this region is given by an average over all of these possibilities. For intermediate energies $|E| \approx 2$ most of the two-particle states are built from one particle in the centre and the second particle close to an edge of the one-particle band. Since there are no contributions from states composed by two particles both located close to an edge of the one-particle band, and furthermore cancellations due to different signs are less important because of different absolute values of the individual curvatures, the typical two-particle level curvatures in these energy ranges are larger than in the centre of the band where a mixing of many different regimes affects the results.

4.2 Influence of the interaction on curvatures

Interactions have a significant influence on the typical two-particle level curvatures. This can be seen by comparing the open symbols in Figure 2 (which are for $U = 0.5$) to the non-interacting case given by the full symbols. The influence of the interaction is shown for disorder strengths $W = 0.75$ and $W = 1.5$. The main observation is that

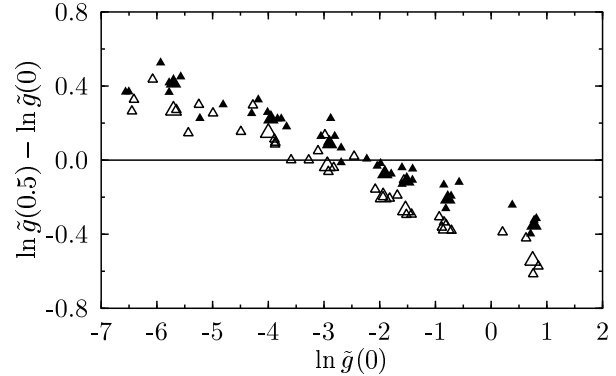


Fig. 3. The difference of the logarithms of the dimensionless curvatures $\tilde{g}(U)$ in rings of size $L = 100$ at interaction strength $U = 0.5$ and at $U = 0$ versus the logarithm of the conductance-like $\tilde{g}(0)$. Full and open triangles are for negative and positive energy, respectively. Large triangles represent averages over the energy ranges $[-2.5 : -1]$ and $[1 : 2.5]$, small triangles are (less precise) averages over narrower energy ranges of width 0.5 within the intervals $[-4 : -1]$ and $[1 : 4]$. The data for disorder strengths between $W = 0.75$ and $W = 1.5$ and the different energies are consistent with two straight lines, one for each sign of the energy.

while at low disorder interactions decrease the curvatures, the latter are increased at higher disorder when the one-particle states are localised. This is a direct confirmation of the prediction by Akkermans and Pichard [24]. A closer look at the data reveals a strong dependence of the effect on the energy regime with a tendency to remove the dip in the curves around $E = 0$.

Although at first glance positive and negative energies seem to show the same behaviour in Figure 2, there are small but significant differences. However, the data obey the symmetry relation $\tilde{c}(U, E) = \tilde{c}(-U, -E)$ because the ensemble of Hamiltonians remains unchanged when both, the sign of the energy and the sign of the interaction are changed. Thus, the data for positive and negative energy should be the same only at $U = 0$, and deviations may occur at finite interaction strength. We have checked that the small difference in our results between positive and negative energy is indeed inverted when the sign of the interaction U is changed, even though the averages have been performed over a limited number of samples. Therefore, it is sufficient to consider only interactions of a definite sign and we restrict ourselves to the case of positive U .

4.3 One parameter scaling

Since the influence of the interaction depends on the mobility of the particles (increase for localised, decrease for metallic samples), it is tempting to define a dimensionless curvature

$$\tilde{g}(U) = \tilde{c}/\Delta_1 \quad (7)$$

where \tilde{c} is the typical curvature at interaction U and $\Delta_1 \approx 2(2t_0 + W)/L$ is the mean one-particle level spacing, and to

plot the interaction-induced change of curvatures not as a function of energy and disorder, but over the conductance-like parameter $\tilde{g}(0)$. The latter is given by the typical non-interacting two-particle curvature \tilde{c} at two-particle energy E in units of Δ_1 and therefore represents an average over the one-particle Thouless-conductances g_1 at the different contributing one-particle energies.

In Figure 3, the difference between the logarithms of the typical absolute values of the dimensionless curvatures with interaction $U = 0.5$ and without interaction are plotted versus the logarithm of the conductance-like parameter $\tilde{g}(0)$ for different energy ranges and disorder strengths W . The large triangles are for the energy intervals $[-2.5 : -1]$ and $[1 : 2.5]$, where the energy dependence of the typical value but also of the shape of the distribution $P(\ln |c|)$ is very small so that statistically reliable and precise data can be obtained by averaging not only over many disorder realisations, but also over a relatively broad energy range. On the other hand, we have omitted the centre of the band in this plot because for strong disorder the distribution $P(\ln |c|)$ shows no significant peak and the error estimates become considerably larger there.

For a given sign of the energy, the data plotted in Figure 3 suggest that the interaction-induced change of the curvatures depends not on the energy and the disorder separately, but on only one parameter which is indeed the conductance-like $\tilde{g}(0)$. This one-parameter scaling is universal within a given sign of the energy. The scaling curves for positive and negative energy differ by a shift of the curvature scale. No change of the scaling curves is observed when the ground state energy is approached. This means that the effect is relevant also for energetically low-lying excitations dominating the transport properties at low temperatures. That interactions indeed reduce or enhance the low-temperature conductance depending on the ratio between disorder and kinetic energy was shown by direct numerical investigations of the energetically lowest many-body states in small disordered two-dimensional systems [27].

The results shown in Figure 3 clearly demonstrate the existence of a critical $\tilde{g}(0) = \tilde{g}_{\text{crit}}$ below which the interaction enhances two-particle level curvatures, and above which the interaction tends to decrease the typical curvatures. This critical value is $\ln \tilde{g}_{\text{crit}} \approx -3$ for positive energies and $\ln \tilde{g}_{\text{crit}} \approx -2.2$ for negative energies¹. Since the level curvature without interaction is related to the conductance of the system, this clearly confirms again that the sign of the interaction-induced change indeed depends on the transport properties of the non-interacting system as predicted [24]. With an estimate of the typical one-particle curvature one finds

$$\tilde{g}(0) \approx (2\pi)^2 \exp(-L/L_1) \quad (8)$$

and the critical conductances above correspond to localisation lengths L_1 which are about 5 to 6 times smaller

¹ The values depend slightly on the averaging procedure. By regarding other averages, we have checked that this does not affect the qualitative results.

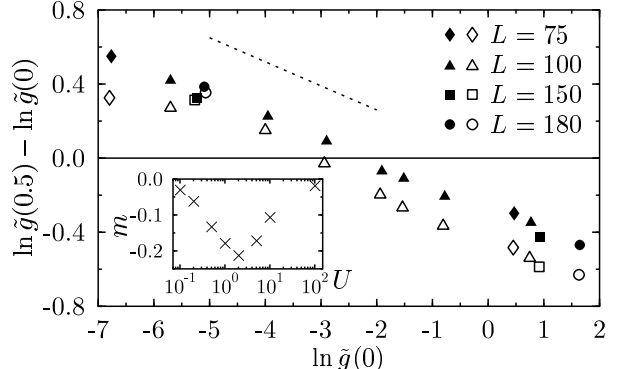


Fig. 4. The difference of the logarithms of the dimensionless curvatures $\tilde{g}(U)$ at interaction strength $U = 0.5$ and $U = 0$ versus the logarithm of $\tilde{g}(0)$. Full symbols represent the energy range $[-2.5 : -1]$, open symbols $[1 : 2.5]$. Different ring sizes $L = 75$ with $W = 0.9$ and $W = 1.8$, $L = 100$ with the same parameters as in Figure 3, $L = 150$ with $W = 0.6$ and $W = 1.2$, $L = 180$ with $W = 0.45$ and $W = 1.1$. The dotted line has the same slope $m \approx -0.13$ as the scaling curves. The inset shows the dependence $m(U)$ of this slope on the interaction strength U .

than the circumference of the ring. Lower conductances $\tilde{g}(0) < \tilde{g}_{\text{crit}}$ correspond to localised states and the enhancement of the curvatures is a consequence of the enhancement of the two-particle localisation length by the interactions proposed by Shepelyansky [12]. Larger conductances $\tilde{g}(0) > \tilde{g}_{\text{crit}}$ can be interpreted as indicating more or less extended one-particle states for which the transport is suppressed by the interactions.

The one-parameter scaling of the change of curvatures with the non-interacting conductance holds also when the system size is varied as shown in Figure 4, where data for different ring sizes between $L = 75$ and $L = 180$ are shown. Within the numerical errors, the data lie on the scaling curve which corresponds to their sign of energy². In the logarithmic representation shown in Figure 4 the scaling curves are very close to straight lines. The slopes $m(U)$ vary between $m = 0$ (at $U = 0$ and $U = \infty$) and the minimal value $m \approx -0.2$ at intermediate interaction strength. Such a scaling law corresponds to a power law dependence

$$\frac{\tilde{g}(U)}{\tilde{g}(0)} \approx \left(\frac{\tilde{g}(0)}{\tilde{g}_{\text{crit}}} \right)^{m(U)}. \quad (9)$$

We have observed interaction-induced changes of the dimensionless curvatures larger than a factor of 2. Thus the effect of the interaction can be rather important.

² The small deviations observed can be explained as follows. For each system size the disorder average has been done over the same set of seeds for the random number generator yielding nice scaling curves in spite of the limited number of different realisations. When comparing different system sizes however it is not possible to use the same realisations and the fluctuations of the data from one set of samples to another one (see Figure 5 below) reduces the relative accuracy of the data points corresponding to different system sizes.

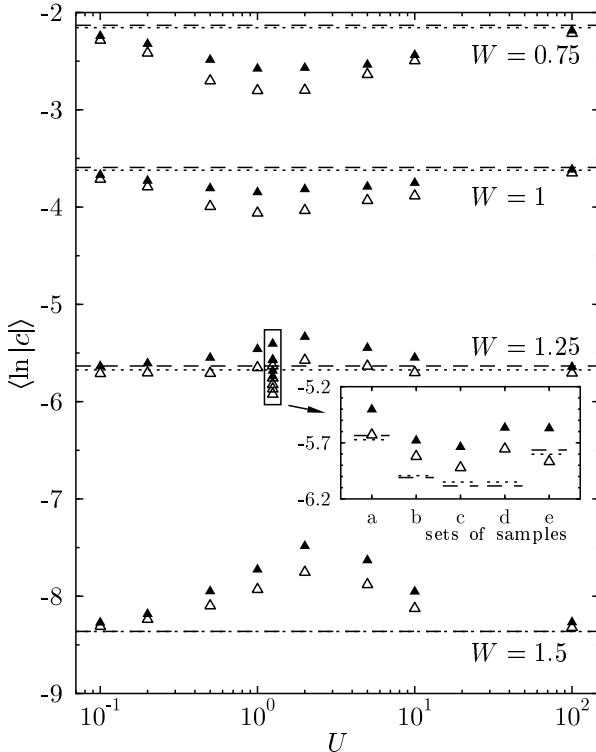


Fig. 5. The typical curvatures as a function of the interaction strength U and rings of size $L = 100$. Symbols show the dependence of $\langle \ln |c| \rangle$ on the interaction, while lines indicate the value at $U = 0$. Full symbols and dashed lines represent the energy range $[-2.5 : -1]$, open symbols and dotted lines are for $[1 : 2.5]$. The inset illustrates the size of the fluctuations due to different disorder realisations.

Our observation is closely related to what is found for the dynamics of two-particle wave-packets [23]. The interaction leads to a slower spreading at short times, before L_1 is reached. For these short times, only a part of the system smaller than L_1 is explored by the particles and their reduced mobility corresponds to the decrease of the curvature in the metallic regime when $\tilde{g}(0)$ is large. On the other hand, above a characteristic time t_1 , a slow interaction assisted propagation continues to increase the size of the wave-packet beyond the non-interacting saturation. This is reminiscent of the increase of curvatures in insulating samples when \tilde{g} is small.

4.4 Duality between weak and strong interaction

For $U = 0$, the eigenstates of the two-particle Hamiltonian are symmetrized products of two one-particle states. Due to the local character of the interaction, this is also the case at infinite interaction U [19, 20], with the only complication that one has to use one-particle eigenstates of the system at $\phi = 1/2$ in order to obtain the two-particle eigenstates at $\phi = 0$. Therefore the typical curvatures are the same in the two limits³. Due to a duality transfor-

³ This is true except for the 'molecular states', where both particles are localised on the same site. For large systems their

tion for the interacting Hamiltonian, the effective interaction matrix elements between the eigenstates at $U = 0$ and $U = \infty$ have the same statistical properties at small U and small $\sqrt{24}t_0^2/U$, respectively. Thus, the spectral correlations are the same in the vicinity of the two limits [19].

The behaviour of the slope of the scaling curves $m(U)$ (inset of Figure 4) shows that the consequences of this duality transformation can also be observed for the curvatures. The full interaction dependence of typical curvatures is presented in Figure 5. As expected from the duality, the influence of the interaction increases up to a value which is of the order $U \sim t_0 = 1$ and returns to the non-interacting value when the interaction is increased further.

As shown in the inset of Figure 5, averages over several different sets of 20 disorder realisations fluctuate significantly (the data at other interaction strength and disorder were calculated with the random seeds from set "a"), and it is difficult to find accurate absolute values for the typical curvatures. However, the interaction dependence is similar for all sets of samples.

5 Distribution of curvatures

Not only the typical value of the two-particle level curvatures but also their probability distribution $P(|c|)^4$ changes as a function of the interaction. Since the spectral statistics has recently been found to be critical in the band centre at $L = L_1$ [19], we now investigate whether a signature of this criticality can be observed in the curvature distribution as well.

In Figure 6 the dependence of $P(|c|)$ on energy is plotted for the disorder $W = 0.5$ chosen such that the one-particle localisation length L_1 in the centre of the band is equal to the system size and thus only the states in the band tails are localised. Picture (a) is for the non-interacting two-particle case and (b) is for the value $U = 1.25$ where the influence of the interaction is close to its maximum.

In the centre and at the edges of the spectrum the typical curvatures are smaller than at other energies (see Figure 2) and the distribution of the curvatures exhibits rather large weights for very small curvatures there. This is most pronounced in the non-interacting case and reduced with interaction. More interestingly, also the shape of the probability distribution changes. This is shown in Figure 7, where the probability distributions $P(k)$ at different energies are compared without and with interaction. Here, we have introduced the normalised curvature $k = c/|\bar{c}|$, with $|\bar{c}|$ being the first moment of the distribution $P(|c|)$.

number is parametrically smaller than the total number of states and their influence can be neglected.

⁴ We discuss now the probability distribution of $|c|$ instead of $\ln |c|$ which, while containing the same information, is more convenient for a comparison of the data with distributions known from the literature.

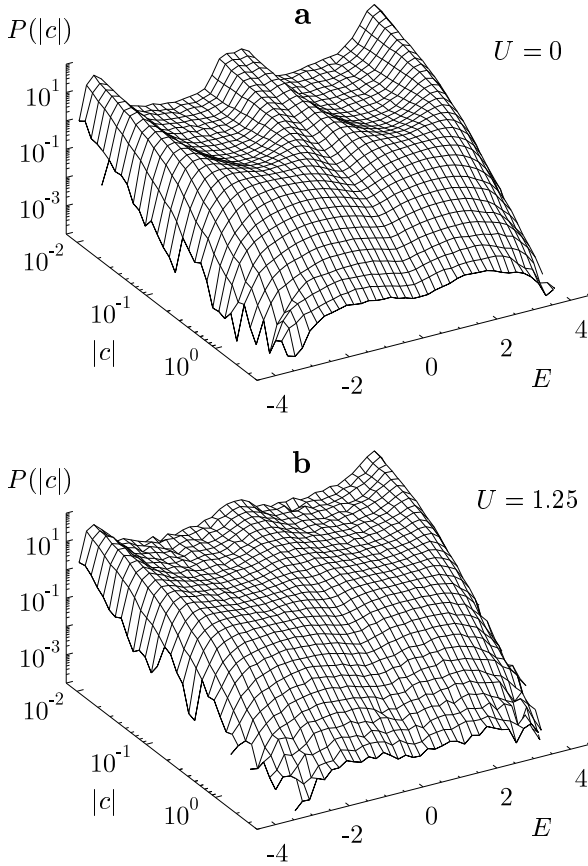


Fig. 6. The distribution $P(|c|)$ for rings of size $L = 100$ at disorder strength $W = 0.5$ (a) without interaction and (b) with interaction $U = 1.25$. The average has been performed over 1000 realisations in the non-interacting and over 100 samples in the interacting case.

5.1 Band centre

In the non-interacting case, no saturation at small curvatures for the distribution in the centre of the band could be found. This indicates that strong deviations from a log-normal distribution persist at small curvatures which arise due to the mixing of different one-particle energy regimes with very different typical curvatures. With interaction the distribution gets closer to the form

$$P_{\text{GOE}}(|k|) = \frac{1}{(1 + |k|^2)^{3/2}}, \quad (10)$$

which was first proposed on the basis of numerical data [28] and later confirmed analytically for the GOE [7]. It was shown that (10) holds in the limit $\phi \rightarrow 0$ even when the external parameter ϕ drives the ensemble into another symmetry class [6, 29].

It has been found recently, that the statistics of eigenvalues in the band centre at intermediate interaction strength is situated between Poisson and GOE and indistinguishable from the critical statistics [19] which is known to hold for several critical systems. Using exactly the same parameters, we tried to find a signature of this

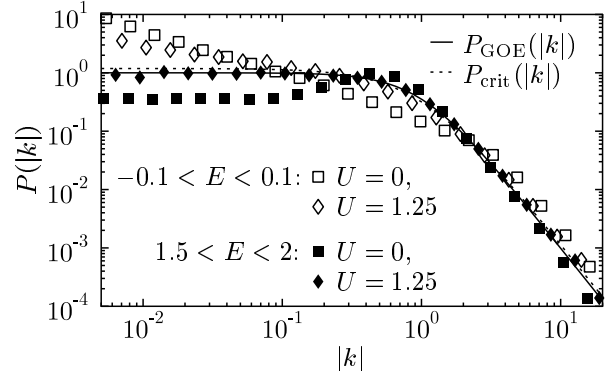


Fig. 7. The probability distribution $P(|k|)$ for a ring of size $L = 100$, averaged over 100 disorder realisations. Open symbols represent the energy range in the centre of the spectrum $|E| < 0.1$, full symbols stand for intermediate positive energy $1.5 < E < 2$. Squares and diamonds are for data points without and with interaction, respectively. The solid and dotted line represents the GOE result (10) and the formula for the critical distribution (11), respectively.

criticality also in the curvature distribution. In Figure 7, we compare our data to the heuristic formula

$$P_{\text{crit}}(|k|) \propto \frac{A}{(1 + |k|^\mu)^{3/\mu}}, \quad (11)$$

which was found to be very close to numerical results for the Anderson transition in three dimensions at the critical point [5] when $\mu \approx 1.58$ was chosen. As can be seen, the difference between the proposed P_{crit} (dotted line) and P_{GOE} (solid line) is very small and our data for the interacting case in the band centre (open diamonds in Figure 7) are inconsistent with both of them. In particular the increase at very small curvature values though weakened, persists with interaction. Thus, while the spectral statistics for the interacting two-particle problem in the band centre [19] is indistinguishable from the one found at the Anderson transition in 3 dimensions [21], the curvature statistics is different from the one found for the Anderson transition in reference [5]. However, the curvature whose properties are predicted to correspond directly to the spectral statistics is of topological origin [24] and differs qualitatively⁵ from the usual curvature considered in this study. It would be interesting to investigate whether the distribution of this topological curvature exhibits criticality like the spectral statistics.

5.2 Finite energy

In the energy interval $[1.5 : 2]$ (full symbols in Figure 7), the situation is completely different. Without interaction,

⁵ It is assumed that the two particles are subject to independent magnetic fluxes ϕ_1 and ϕ_2 . The topological curvatures [24] of the two-particle energy levels E_j are then defined as $c_j^{\text{top}} = \partial^2 E_j / \partial \phi_1 \partial \phi_2|_{\phi_1=\phi_2=0}$.

the distribution exhibits a relative minimum at small curvature and a distinct peak close to the mean curvature, which becomes even more pronounced when the disorder is further decreased. Such a behaviour is known to occur for the ballistic regime in the one-particle curvature statistics [3]. In one-dimensional systems the mean free path is of the order of the localisation length and thus of the order of the system size for the chosen parameters. Therefore, the one-particle dynamics is close to ballistic and the non-interacting two-particle curvatures in the given energy range are dominated by the properties of the one-particle curvatures. With interaction, the distribution becomes indistinguishable from the random matrix theory result (10) which is known to be valid in the diffusive regime of the one-particle problem. This suggests that the electron-electron scattering makes the originally ballistic dynamics diffusive and represents a way to understand why the typical curvatures (and the mobility of the particles) are reduced by interactions in this regime.

The shape of the probability distribution at the edges of the two-particle band, where localised states dominate, is close to the one shown in Figure 7 for the band centre (open symbols). The interaction drives the distribution towards the GOE form, which is a consequence of the mixing of one-body states by the interaction. At stronger disorder or larger system size, eventually all of the states are localised and the probability distribution of the two-particle level curvatures is the same in all energy ranges.

6 Conclusions

We have studied numerically the two-particle level curvatures in disordered chains as a function of the strength of an on-site interaction between the particles. This paper contains two main results: Firstly, we found that the typical value of the curvatures is increased by the interactions in the localised and reduced in the metallic regime, respectively. In the localised case, this is a consequence of Shepelyansky's delocalisation effect [12] while in the metallic case electron-electron scattering reduces the mobility of the particles. Our observation represents the first direct confirmation of a recent analytical prediction [24]. Secondly, we have presented evidence for a one-parameter scaling of the interaction-induced change of the curvatures with a non-interacting conductance. The critical curvature where the data are not affected by the interaction corresponds to $L/L_1 \approx 6$. While the precise relation between many-particle level curvatures and the conductance should be studied in detail, this suggests that the conductance of metals is reduced by the influence of electron-electron interactions, while the conductance of insulators (which is exponentially suppressed by the disorder), may be enhanced by the interactions. The same conclusion is reached in a study of the dynamics of two-particle wave-packets [23].

In addition, we have also found the signature of the duality transformation between small and very strong interaction [19] in the curvatures and investigated the probability distribution of the two-particle level curvatures in

detail. As expected, the distributions are always driven towards the random matrix theory result by the interactions, but starting from different non-interacting distributions depending on the energy range. This further supports that the different consequences of the presence of interactions in metallic and localised regimes, respectively, may be relevant for the conductance of real systems.

The level curvatures of the interacting two-particle system yield relevant informations like the change of sign of the interaction effect which cannot be obtained directly from studies of the spectral statistics. This is in contrast to the one-particle problem where curvature and spectral statistics are closely related.

We acknowledge stimulating discussions with Gert-Ludwig Ingold, Jean-Louis Pichard and Xavier Waintal. The numerical calculations were partly done on the IBM SP2 at the Leibniz-Rechenzentrum München.

References

1. J.T. Edwards, D.J. Thouless, *J. Phys. C* **5**, 807 (1972).
2. D.J. Thouless, *Phys. Rep.* **13**, 93 (1974).
3. D. Braun, E. Hofstetter, A. MacKinnon, G. Montambaux, *Phys. Rev. B* **55**, 7557 (1997).
4. K. Życzkowski, L. Molinari, F.M. Izrailev, *J. Phys. I France* **4**, 1469 (1994).
5. C.M. Canali, C. Basu, W. Stephan, V.E. Kravtsov, *Phys. Rev. B* **54**, 1431 (1996).
6. D. Braun, G. Montambaux, *Phys. Rev. B* **50**, 7776 (1994).
7. F. von Oppen, *Phys. Rev. E* **51**, 2647 (1995).
8. M. Titov, D. Braun, Y.V. Fyodorov, *J. Phys. A* **30**, L339 (1997).
9. U. Eckern, P. Schwab, *Adv. Phys.* **44**, 387 (1995).
10. *Correlated Fermions and Transport in Mesoscopic Systems*, edited by T. Martin, G. Montambaux, J. Trân Thanh Vân (Editions Frontières, Gif-sur-Yvette, 1996).
11. P. Schmitteckert, R.A. Jalabert, D. Weinmann, J.-L. Pichard, *Phys. Rev. Lett.* (to be published).
12. D.L. Shepelyansky, *Phys. Rev. Lett.* **73**, 2067 (1994).
13. Y. Imry, *Europhys. Lett.* **30** 405 (1995).
14. K. Frahm, A. Müller-Groeling, J.-L. Pichard, D. Weinmann, *Europhys. Lett.* **31**, 169 (1995).
15. D. Weinmann, A. Müller-Groeling, J.-L. Pichard, K. Frahm, *Phys. Rev. Lett.* **75**, 1598 (1995).
16. F. von Oppen, T. Wettig, J. Müller, *Phys. Rev. Lett.* **76**, 491 (1996).
17. F. von Oppen, T. Wettig, *Europhys. Lett.* **32**, 741 (1995).
18. D. Weinmann, J.-L. Pichard, *Phys. Rev. Lett.* **77**, 1556 (1996).
19. X. Waintal, D. Weinmann, J.-L. Pichard, TIP II, cond-mat/9801134, *Eur. Phys. J. B* (to be published).
20. I.V. Ponomarev, P.G. Silvestrov, *Phys. Rev. B* **56**, 3742 (1997).
21. D. Braun, G. Montambaux, M. Pascaud, *Phys. Rev. Lett.* **81**, 1062 (1998).
22. X. Waintal, J.-L. Pichard, TIP I, cond-mat/9706258, *Eur. Phys. J. B* (to be published).
23. S. De Toro Arias, X. Waintal, J.-L. Pichard, TIP III, cond-mat/9808136.

24. E. Akkermans, J.-L. Pichard, Eur. Phys. J. B 1, 223 (1998).
25. A. Wobst, Diplomarbeit, Universität Augsburg (1998).
26. J.-L. Pichard, in *Quantum Coherence in Mesoscopic Systems*, ed. by B. Kramer, NATO ASI Vol. B 254 (Plenum, New York, 1991).
27. T. Vojta, F. Epperlein, M. Schreiber, cond-mat/9806194.
28. J. Zakrzewski, D. Delande, Phys. Rev. E **47**, 1650 (1993).
29. Y.V. Fyodorov, H.-J. Sommers, Phys. Rev. E **51**, R2719 (1995).